Free energy of ion hydration: Interface susceptibility and scaling with the ion size

Mohammadhasan Dinpajooh[1] and Dmitry V. Matyushov[2, a)]
[1)] *Department of Chemistry & Biochemistry, Arizona State University, PO Box 871504, Tempe, Arizona 85287*
[2)] *Department of Physics and Department of Chemistry & Biochemistry, Arizona State University, PO Box 871504, Tempe, Arizona 85287*

Free energy of solvation of a spherical ion in a force-field water is studied by numerical simulations. The focus is on the linear solvation susceptibility connecting the linear response solvation free energy to the squared ion charge. Spherical hard-sphere solutes, hard-sphere ions, and Kihara solutes (Lennard-Jones modified hard-sphere core) are studied here. The scaling of the solvation susceptibility with the solute size significantly deviates from the Born equation. Using empirical off-set corrections of the solute size (or the position of the first peak of the solute-solvent distribution function) do not improve the agreement with simulations. We advance a new perspective on the problem by deriving an exact relation for the radial susceptibility function of the interface. This function yields an effective cavity radius in the Born equation calculated from the solute-solvent radial distribution function. We find that the perspective of the local response, assuming significant alteration of the solvent structure by the solute, is preferable compared to the homogeneous approximation assuming intact solvent structure around the solute. The model finds a simple explanation of the asymmetry of hydration between anions and cations in denser water shells around anions and smaller cavity radii arising from the solute-solvent density profiles.

I. INTRODUCTION

The free energy F_0 of solvating an ion in a polar molecular liquid is usually described by the linear-response equation connecting it to the ion charge q through the solvation susceptibility χ

$$F_0 = -\tfrac{1}{2}\chi q^2. \tag{1}$$

Many computer simulation studies have shown that the quadratic scaling with the charge is fulfilled remarkably well and solvation can be described as linear.[1–4] Given this success, the main focus, in particular in applications,[5–7] is to link the solvation susceptibility χ to the properties of the ion and the solvent. This study is mostly concerned with the problem of the scaling of χ with the size of a spherical solute. We show that χ can be represented as a one-dimensional radial integral of the local susceptibility function $\chi_0(r)$. An exact formula for $\chi_0(r)$ is derived [Eq. (21)] and evaluated by numerical simulations.

The Born model of ion solvation represents the solvent by a continuum polarizable medium and the ion by a spherical cavity with the radius a carved in the continuum.[8] The resulting solvation susceptibility is given by the relation

$$\chi_{\rm B} = \frac{1}{a}\left(1-\frac{1}{\epsilon}\right). \tag{2}$$

The model thus factors χ into the geometric cavity parameter a^{-1} and the longitudinal susceptibility[9,10] of the bulk polar solvent $\propto (1-\epsilon^{-1})$ defined by its dielectric constant ϵ. It is typically assumed that the cavity radius a can be connected to the solute radius R_0 by a distance off-set δ,[11,12]

$$a = R_0 + \delta. \tag{3}$$

We show here that this phenomenological relation does not stand the test against numerical simulations in a sufficiently broad range of solute sizes. We propose instead a new equation for the cavity radius in terms of the solute-solvent radial distribution function.

The dependence on the solvent polarity is more complex than prescribed by the Born equation when the assumption of the continuum polarizable solvent is lifted and finite size of the solvent molecules is explicitly included. For instance, solvation of ions by a fluid of dipolar hard spheres with diameter σ can be calculated in the mean-spherical approximation (MSA). One gets for the cavity radius in the Born equation[13] $a(P,T) = R_{0s} - \Delta(P,T)$. Here, $R_{0s} = R_0 + \sigma/2$ is the distance of the closest approach of the solvent to the solute repulsive core, which is also the position of the first maximum $r_{\rm max}$ of the solute-solvent pair distribution function. The MSA solution thus predicts $\delta = \sigma/2 - \Delta(P,T)$ in Eq. (3), where $\Delta(P,T)$, by which R_{0s} is reduced, is the length of longitudinal dipolar correlations in the bulk solvent.[9,10] Based on this theoretical prediction and fitting the experimental data,[11] it is commonly assumed that the phenomenological cavity radius a should fall between R_0 and R_{0s}.[14] For "soft" solutes, the position of the first maximum $r_{\rm max}$ of the solute-solvent radial distribution function replaces R_{0s}.[15,16]

The parameter $\Delta(P,T)$ carries the dependence on the thermodynamic state of the solvent, which is indicated by its dependence on pressure P and temperature T. This particular solution exemplifies the general result that the cavity radius cannot be defined as a constant even for a

[a)] Electronic mail: dmitrym@asu.edu

given solvent/solute combination and needs instead to be a function of the solvent thermodynamic state.[16,17] Assuming $a = Const$ gives unreliable values for the solvation entropy and, most likely, for other thermodynamic derivatives of the solvation free energy.[16,18–20] What we show here is that the dependence of the cavity size on both the thermodynamic state of the solvent and on the solute-solvent potential can be accommodated in terms of the solute-solvent radial distribution function.

The specific problem of ion hydration presents additional complications. The solvation susceptibility χ in Eq. (1) gains an additional dependence on the sign of q, even though the linear scaling $F_0 \propto q^2$ is preserved for the positive and negative charges separately.[2,16,18] In addition, spontaneous polarization of hydration shells around solutes carrying no charge creates a non-zero electrostatic potential within a zero-charge solute.[21] A solute of zero charge does not polarize the solvent in the standard dielectric theories. This is because of the assumption that the interface susceptibility is identical to the susceptibility of the isotropic bulk liquid (homogeneous approximation discussed below). In fact, inserting even a charge neutral solute into an isotropic solvent breaks the isotropic symmetry. Zero polarization at zero charge is not required by symmetry any longer and can be violated depending on the solvent, as indeed happens for aqueous solutions.

In the case of water, a nonpolar[18,22] or a hard-sphere (HS)[21] solute carrying no charge produces a spontaneous polarization of the interface with a resulting nonzero potential $\langle\phi\rangle_0$ at $q = 0$ (subscript "0"). The magnitude of $\langle\phi\rangle_0$ is hard to establish experimentally even at a planar interface,[7,23] and the results of simulations show a significant dependence of $\langle\phi\rangle_0$ on the adopted force field.[4,24–27] The sign of $\langle\phi\rangle_0$ also depends on the definition of the cavity potential and whether cavity repulsion is applied to water's hydrogen atoms.[28] Given these uncertainties, we do not discuss $\langle\phi\rangle_0$ in this paper, focusing instead on the charge susceptibility χ in Eq. (1).

The positive sign of $\langle\phi\rangle_0$ inside HS and Lennard-Jones (LJ) cavities in point-charge force field water was calculated from a number of previous simulations[4,21] and also, for an extended range of radii, in our simulations as shown by Fig. S1 in the Supplementary Material (SM)[29]. It adds negative solvation free energy to an anion. However, although accounting for some solvation asymmetry, this shift of the potential is not sufficient and lower values of the cavity radii for anions compared to cations are required in the Born solvation susceptibility χ_B in Eqs. (1) and (2).[4] Along the same lines, we find here that the second cumulant $\langle(\delta\phi)^2\rangle_0$, which is the main contributor to the solvation free energy,[4] is asymmetric between cations and anions, as first discussed by Hummer *et al.*[2] We attribute this asymmetry to different local densities of water around ions of opposite charge. Once the density profile of the interface is accommodated into the definition of the cavity radius (Eq. (18) below), the Born linear susceptibility successfully accounts for the scaling with the solute size produced by the simulations.

II. GENERAL FORMALISM

The linear-response free energy of ion solvation can be written as the multipolar expansion of the solute-solvent Coulomb potential in solvent multipoles[30,31]

$$F_0 = -\tfrac{1}{2}\int \left[\mathbf{E}_0 \cdot \langle\mathbf{P}\rangle_E + \tfrac{1}{3}\nabla\mathbf{E}_0 : \langle\mathbf{Q}\rangle_E + \dots\right] d\mathbf{r}. \quad (4)$$

Here, $\mathbf{E}_0$ is the electric field of the ion charges and $\mathbf{P}$ and $\mathbf{Q}$ are the dipolar and quadrupolar (defined according to Ref. 31) polarization densities of the solvent, respectively. The brackets $\langle\dots\rangle_E$ denote the two polarization fields in equilibrium with the solute.

The quadrupolar term is potentially important for hydration because of a large non-axial quadrupole moment of the water molecules reflecting its charge asymmetry. We will, however, drop it from our discussion here and focus solely on the dipolar polarization of the interface. This assumption is justified for relatively large solutes since quadrupolar solvation decays faster with the solute size than dipolar solvation.[32] Our starting point is, therefore, the linear solvation free energy[33] written as the integral of the electric field of an ion with the dipolar equilibrium polarization density

$$F_0 = -\tfrac{1}{2}\int \mathbf{E}_0 \cdot \langle\mathbf{P}\rangle_E d\mathbf{r}. \quad (5)$$

Returning to the symmetry arguments presented above, the charge inversion $q \to -q$ results in $\mathbf{E}_0 \to -\mathbf{E}_0$, which reverses the sign in Eq. (5). The same reversal can be achieved by flipping all the dipoles in the solvent $\mathbf{m}_j \to -\mathbf{m}_j$ thus producing $\mathbf{P} \to -\mathbf{P}$. The Hamiltonian of the liquid in the external field, $H = H_0 - \int \mathbf{E}_0 \cdot \mathbf{P} d\mathbf{r}$, will remain invariant to the simultaneous $q \to -q$ and $\mathbf{P} \to -\mathbf{P}$ transformation when the unperturbed Hamiltonian H_0 is invariant to $\mathbf{P} \to -\mathbf{P}$. This is the case with the homogeneous approximation, which assumes that the solute does not strongly perturb the solvent and its response can be given in terms of response functions of the homogeneous solvent (Born formula, Eq. (2)). This implies that H_0 is effectively the Hamiltonian of the bulk solvent. The transformation $\mathbf{P} \to -\mathbf{P}$ does not change any properties of an isotropic liquid. Therefore, the solvation susceptibility in this homogeneous approximation should be invariant to the $q \to -q$ transformation.

Alternatively, when the isotropic symmetry of the homogeneous solvent is broken by the repulsive core of the solute, the dipole flip $\mathbf{m}_j \to -\mathbf{m}_j$ in the interface will produce a physically distinct configuration even at $q = 0$. In other words, the Hamiltonian H_0, which includes the repulsive core of the solute, is not invariant to $\mathbf{P} \to -\mathbf{P}$. One therefore expects that the observables measured even in the linear response will not demonstrate the $q \to -q$ invariance, in contrast to the models

based on the homogenous approximation. This feature is captured by the local approximation introduced below to contrast with the homogeneous approximation of the standard dielectric theories. We stress that the $q \to -q$ asymmetry does not violate the quadratic scaling of the solvation free energy with the ion charge. It only implies that the solvation susceptibility χ in Eq. (1) should be given different values for positive and negative ions.

We also note that the quadrupolar polarization in Eq. (4) eliminates the symmetry to the simultaneous transformation $q \to -q$ and $\mathbf{m}_j \to -\mathbf{m}_j$. Therefore, this term, when included, will also contribute to the asymmetry of the observables to the charge inversion $q \to -q$. This is what is often referred to as charge asymmetry of water contributing to solvation asymmetry.[18,34,35] However, a potentially more important cause of solvation asymmetry is the difference in the density profiles of water around cations and anions, which is ultimately related to the asymmetric molecular shape and asymmetric distribution of molecular charge in water, but cannot be pinned down to one specific molecular property, such as molecular quadrupole. We present below arguments suggesting that this is essentially a "zero-order" effect, which accounts for most of the solvation asymmetry in terms of a density-weighted effective cavity radius of ion solvation.

A. Approximate interface susceptibilities

The integral in Eq. (5) can be re-written, in the linear response, in terms of two fields and a two-point correlation function of the polarization field

$$\chi_{0s}^{\alpha\beta}(\mathbf{r}', \mathbf{r}'') = 4\pi\beta\langle\delta P_\alpha(\mathbf{r}')\delta P_\beta(\mathbf{r}'')\rangle_0, \tag{6}$$

where the average $\langle\dots\rangle_0$ is now taken over the configurations of water around the repulsive core of the solute carrying no charge and δX for a spatially varying field X, such as δP_α, is used here to describe deviations from statistically average values. Equation (5) turns into the following relation

$$F_0 = -\frac{1}{8\pi}\int E_{0\alpha}(\mathbf{r}')E_{0\beta}(\mathbf{r}'')\chi_{0s}^{\alpha\beta}(\mathbf{r}', \mathbf{r}'')\, d\mathbf{r}' d\mathbf{r}''. \tag{7}$$

Here and in Eq. (6) α, β subscripts denote Cartesian projections and the summation over the common indexes is assumed.

The fundamental complexity of the solvation problem arises from the fact that the second-rank tensor susceptibility $\boldsymbol{\chi}_{0s}$ defined by Eq. (6) is a three-particle correlation function involving correlations of translations and orientations of two water molecules with the position and orientation of the solute. This difficulty has mostly been resolved over many years of studies by attempting to reformulate the problem in terms of two-particle correlation functions.[36] Two possible general directions for formulating such approximations can be identified. They can be labelled as either (i) a "homogeneous" approximation or (ii) a "local" approximation (to which all models with the distance-dependent dielectric constant can be assigned[37]).

In the homogeneous approximation, one assumes that the water-water correlations are not significantly broken by the solute and one can replace $\boldsymbol{\chi}_{0s}(\mathbf{r}', \mathbf{r}'')$, depending on positions of two water molecules $\mathbf{r}'$ and $\mathbf{r}''$ separately, with a homogeneous susceptibility $\boldsymbol{\chi}_s(\mathbf{r}' - \mathbf{r}'')$ depending only on $\mathbf{r}' - \mathbf{r}''$ (isotropic liquids)[38]

$$\boldsymbol{\chi}_{0s}(\mathbf{r}', \mathbf{r}'') = \theta_V(\mathbf{r}')\theta_V(\mathbf{r}'')\boldsymbol{\chi}_s(\mathbf{r}' - \mathbf{r}''), \tag{8}$$

where $\theta_V(\mathbf{r})$ is a step function equal to zero inside the solute and equal to unity otherwise. It specifies the volume V of the solvent from which the homogeneous solvent response is calculated.

The alternative, local approximation would take the opposite view that inserting a solute produces a major alteration of the water structure. Therefore, in this view, the structure of the interface, and not the correlations present in bulk water, is of main significance for the hydration thermodynamics. One then can go to the limit of neglecting the correlations between different water molecules in the interface altogether and replace $\boldsymbol{\chi}_{0s}(\mathbf{r}', \mathbf{r}'')$ with a local function[39]

$$\boldsymbol{\chi}_{0s}(\mathbf{r}', \mathbf{r}'') = \delta\left(\mathbf{r}' - \mathbf{r}''\right)\boldsymbol{\chi}_0(\mathbf{r}'). \tag{9}$$

While each of these assumptions, Eqs. (8) and (9), involve approximations, both have been widely used since they significantly simplify the problem. In terms of going beyond the static dielectric constant of a bulk liquid, the homogeneous and local approximations correspond to k-dependent, $\epsilon(k)$,[40] and distance-dependent, $\epsilon(r)$, dielectric constants, respectively. The wavevector-dependent dielectric constant $\epsilon(k)$ of a bulk material has a solid foundation in the Kubo linear response theory.[41] On the contrary, $\epsilon(r)$ was originally introduced as a phenomenological prescription to account for inhomogeneity of the interface[5,42,43] and has only recently received microscopic-based definitions for spherical,[39,44,45] planar,[39,46–49] or cylindrical[45] interfacial geometries.

What we want to accomplish here is to give a clear mathematical foundation of using the distance-dependent polarization susceptibility $\chi_0(r)$ of the interface. This study is limited to spherical solutes and, therefore, only the radial, angular-symmetric susceptibility is considered. We in fact find that this susceptibility provides a good reference point for describing ion solvation upon which more advanced theoretical algorithms can be developed. We first apply each of two closures, homogeneous and local, to the linear-response solvation free energy in Eq. (7) with the goal of arriving at the Born equation. We then provide in Section II C an exact analytical solution for $\chi_0(r)$ in terms of binary correlations accessible from numerical simulations.

The free energy in the homogeneous approximation is the convolution of two electric fields at points $\mathbf{r}'$ and $\mathbf{r}''$

with the susceptibility function depending on $\mathbf{r}' - \mathbf{r}''$. These types of integrals are best taken in the inverted $\mathbf{k}$-space, which both eliminates the convolution and allows one to reduce the problem to scalar susceptibility projections. In the case of a spherical ion, this latter reduction is the consequence of the radial symmetry of the electric field which couples to the longitudinal projection of the susceptibility[50,51]

$$F_0 = -\frac{1}{2}\int \frac{d\mathbf{k}}{(2\pi)^3}\left|\tilde{E}_0^L(k)\right|^2 \chi_s^L(k). \tag{10}$$

Here, $\tilde{E}_0^L = \hat{\mathbf{k}}\cdot\tilde{\mathbf{E}}_0$, $\hat{\mathbf{k}} = \mathbf{k}/k$ is the longitudinal projection of the Fourier transform $\tilde{\mathbf{E}}_0$ of the electric field of the ion taken outside its repulsive core, $\theta_V\mathbf{E}_0$. Its longitudinal character, stressed by the subscript "L", is the combined result of the longitudinal field $\mathbf{E}_0$ and the spherical symmetry of the ion's repulsive core assumed here. Non-spherical repulsive cores require both longitudinal and transverse response projections to determine the free energy.[36,51]

The longitudinal susceptibility[10,52,53] in Eq. (10) is given in terms of the longitudinal structure factor of the polar liquid[54]

$$\chi_s^L(k) = (3y/4\pi)S^L(k), \tag{11}$$

where $y = (4\pi/9)\beta m^2\rho$ is the usual parameter of the dipolar density of molecular dielectrics[55] carrying molecular dipoles m and having the number density $\rho = N/V$. The longitudinal structure factor $S^L(k)$ is given in terms of unit-vector orientations $\hat{\mathbf{e}}_i$ and positions $\mathbf{r}_i$ of molecular dipoles in the bulk

$$S^L(k) = \frac{3}{N}\sum_{i,j}\left\langle(\hat{\mathbf{e}}_i\cdot\hat{\mathbf{k}})(\hat{\mathbf{k}}\cdot\hat{\mathbf{e}}_j)e^{i\mathbf{k}\cdot\mathbf{r}_{ij}}\right\rangle, \tag{12}$$

where $\mathbf{r}_{ij} = \mathbf{r}_i - \mathbf{r}_j$ and the statistical average is over the configurations of N molecules of the bulk liquid occupying the volume V.

We can now apply the $\mathbf{k}$-space field of the spherical ion, $\tilde{E}_0^L(k) = (4\pi iq/k)j_0(ka)$ ($j_n(x)$ is the spherical Bessel function of order n[56]), and note that $\chi^L(k)$ depends on the product of k and the solvent molecular diameter σ. The solvation susceptibility χ in Eq. (1) takes the form

$$\chi = \frac{2\chi_B}{\pi}\int_0^\infty dx j_0(x)^2\chi^L\left(x\frac{\sigma}{a}\right)/\chi^L(0), \tag{13}$$

where χ_B is the Born susceptibility in Eq. (2). The dependence of the longitudinal susceptibility on the wavevector k can be neglected when $\sigma \ll a$. The function $\chi^L(x\sigma/a)$ can be then replaced with $\chi^L(0) = (4\pi)^{-1}(1-\epsilon^{-1})$, with the result $\chi = \chi_B$. More generally, $\chi^L(x\sigma/a)$ can be expanded in σ/a at $\sigma \ll a$ and one gets the solvation susceptibility in the form $\chi = \chi_B\sum_n c_n(\sigma/a)^n$ consistent with the MSA solution.[13]

The solution for the solvation free energy simplifies even further in the local approximation given by Eq. (9). The solvation susceptibility in Eq. (1) becomes

$$\chi = \int_0^\infty \frac{dr}{r^2}\chi_0(r). \tag{14}$$

From this equation, one arrives at the Born result if one assumes $\chi_0(r) = \theta(r-a)(1-\epsilon^{-1})$, where $\theta(x)$ is the Heaviside function. More generally, from Eqs. (6) and (9) and with the account for the radial symmetry of the ion field, $\chi_0(r)$ is a scalar function given by the relation

$$\chi_0(r) = 4\pi\beta\langle\delta P_r(r)\delta M_r\rangle_0. \tag{15}$$

Here, $P_r = \hat{\mathbf{r}}\cdot\mathbf{P}$, $\hat{\mathbf{r}} = \mathbf{r}/r$ and $M_r = \sum_j \mathbf{m}_j\cdot\hat{\mathbf{r}}_j$ is the sum of all radial projections of the liquid dipoles assuming that the spherical ion is positioned at the origin of the laboratory coordinate frame.[31]

Equation (15) is the direct consequence of the local response approximation in Eq. (9) and is similar in structure to analogous relations recently proposed in the literature.[44,48] The local approximation is a useful device for deriving analytical approximations, but is not required for producing the interface susceptibility from simulation trajectories. In section II C, we derive an alternative, and exact, equation based on the correlation of fluctuations of the radial polarization field and the solvent "reaction"[57] potential at the position of the ion. The connection between χ and $\chi_0(r)$ in Eq. (14) is also exact in that formulation and does not require the local assumption of Eq. (9).

B. Cavity radius

The average over the solvent configurations around the solute excluding the solvent from its volume, $\langle\ldots\rangle_0$, in Eq. (15) can be expressed in terms of the three-particle distribution function $g(\mathbf{r}_1\omega_1, \mathbf{r}_2\omega_2)$ representing the probability to find two water molecules at the positions $\mathbf{r}_1$ and $\mathbf{r}_2$ and orientations of their dipole ω_1 and ω_2 with the solute considered as the center of the laboratory coordinate frame.[31] The average can be taken by employing the Kirkwood superposition approximation, $g(\mathbf{r}_1\omega_1, \mathbf{r}_2\omega_2) \simeq g_{0s}(\mathbf{r}_1\omega_1)g_{ss}(\mathbf{r}_{12}\omega_1\omega_2)g_{0s}(\mathbf{r}_2\omega_2)$, where g_{0s} and g_{ss} stand for the solute-solvent and solvent-solvent distribution functions, respectively. This derivation is given in SM.[29] The closed-form expression for the local susceptibility $\chi_0(r)$ can be achieved by taking the long-range, continuum limit for the longitudinal structure factor $S^L(k) \to S^L(0)$ appearing in the integral representation of $\chi_0(r)$. The $k = 0$ value of the structure factor produces the standard longitudinal dielectric susceptibility, $S^L(0) \propto (1-\epsilon^{-1})$, with the final result

$$\chi_0(r) = \left(1-\epsilon^{-1}\right)\left[g_{0s}(r)\right]^2. \tag{16}$$

Here, $g_{0s}(r)$ is the solute-solvent radial pair distribution function.

The radial susceptibility $\chi_0(r)$ represents the longitudinal response function of radial hydration shells and

therefore can be connected to a radial, distant-dependent dielectric constant of the interface

$$\epsilon_r(r)^{-1} = 1 - \chi_0(r). \tag{17}$$

It is easy to see that this function crosses zero and becomes negative in the vicinity of the peaks of $g_{0s}(r)$ in Eq. (16).[48] The radial dielectric constant itself hardly has any significant physical meaning and only the radial longitudinal susceptibility $\chi_0(r)$ represents the longitudinal polarization response of the interface. This notion also implies that attempts of producing radial dielectric constants $\epsilon_r(r)$, and perhaps more generally position-dependent dielectric constants, in terms of phenomenological smooth functions have no support of microscopic theories.[39]

When Eq. (16) for $\chi_0(r)$ is substituted into Eq. (14), one arrives at the standard Born equation with the cavity radius defined as

$$\frac{1}{a} = \int_0^\infty \frac{dr}{r^2} \left[g_{0s}(r)\right]^\alpha, \tag{18}$$

where $\alpha = 2$ is required by Eq. (16). Our calculations of the response from simulations below show that this choice of α, following from the local approximation, overestimates the oscillatory behavior of $\chi_0(r)$ and instead $\alpha < 1$ is required to reproduce the simulations.

Berne and co-workers[58] suggested $\alpha = 1$ in Eq. (18) whereas Linder and Hoernschemeyer[17] used $3g_{0s}(r)/r^4$ as the integrand in Eq. (18) to define $1/a^3$. All these original propositions were given without proof, although representing the electrostatic energy by a sum over a dipolar lattice can be used to justify[59] $\alpha = 1$ in Eq. (18). A dipolar lattice of course does not display an interfacial density alteration and is not a good model for testing the cavity concepts. On the other hand, our empirical α-scaling follows from the exact formula for $\chi_0(r)$ taken from Eq. (21) derived in the next section and used in Eq. (14), combined with its direct calculation from simulation trajectories.

One can use Eq. (18) for a crude estimate of the scaling of the solvation free energy with the cavity radius. This follows from the $r \to \infty$ asymptote[31] of $g_{0s}(r) = 1 + h_{0s}(r)$: $h_{0s}(r) \propto r^{-1}$. If $h_{0s}(r)$ dominates in $g_{0s}(r)$ near the contact, one can replace $[g_{0s}(r)]^\alpha$ with $\theta(r-a)[h_{0s}(r)]^\alpha$ in Eq. (18) to obtain $F_0 \propto 1/a^{\alpha+1}$. The power law decay in fact gives a reasonable account of our simulation data (Fig. 3 below). However, the complete integral representation for the cavity radius in terms of Eq. (18) is more consistent with simulations. Note also that Eq. (18) yields the standard definition of the cavity size for a structureless continuum interfacing the solute when the solute-solvent pair distribution function reduces to the Heaviside function, $g_{0s}(r) = \theta(r-a)$.

C. Exact interface susceptibility

In the previous section, we have discussed two approaches to handle the inhomogeneous character of the interfacial response of a polar solvent in terms of the distribution functions formalisms of liquid-state theories. Here, we provide an exact representation of the interface susceptibility $\chi_0(r)$ in terms of correlation functions accessible from configurations produced by numerical simulations.

The starting point of our analysis is the recognition of the fact that the electric field of the ion $\mathbf{E}_0$ has longitudinal symmetry, implying that its curl is identically zero,[30] $\nabla \times \mathbf{E}_0 = 0$. The symmetry of the field of charges imposes a corresponding symmetry on the dipolar polarization density $\mathbf{P}$, which should be longitudinal as well.[60] The longitudinal component of the polarization density $\mathbf{P}_L$ is directly related to the electrostatic potential Φ_p produced by the charges of the solvent[61,62]

$$4\pi\mathbf{P}_L = \nabla\Phi_p. \tag{19}$$

This connection can be productively used to derive the exact relation for the interface susceptibility in Eq. (14), which can be re-written as follows

$$\chi_0(r) = (r^2/q) \int \chi_{0s}^{r\beta}(\mathbf{r},\mathbf{r}') E_{0\beta}(\mathbf{r}') d\mathbf{r}', \tag{20}$$

where $\chi_{0s}^{r\beta}$ is given by Eq. (6) and the "r" superscript denotes the radial projection: $\chi_{0s}^{r\beta} = \hat{r}^\alpha \chi_{0s}^{\alpha\beta}$. Note that this form of $\chi_0(r)$ in Eq. (14) is exact and does not require the local approximation of Eq. (9).

By substituting Eq. (19) in place of the δP_β projection in Eq. (6) and integrating by parts, one can eliminate the volume integral in Eq. (20) by noting that $\nabla \cdot \mathbf{E}_0(\mathbf{r}) = 4\pi q\delta(\mathbf{r})$. The final result for the interfacial susceptibility is

$$\chi_0(r) = -4\pi\beta r^2 \langle \delta P_r(r) \delta\phi \rangle_0. \tag{21}$$

Here, $\phi = \Phi_p(0)$ is the electrostatic potential produced by the solvent at the position of the ion at the center of the solute and $\delta\phi = \Phi_p(0) - \langle\Phi_p(0)\rangle$. Further, ϕ can be directly related to the molecular charge density of the solvent $\rho_s' = \rho_s(\mathbf{r}')$ as follows

$$\phi = \int \frac{\rho_s'}{r'} d\mathbf{r}' = \sum_j \frac{q_j}{r_j}, \tag{22}$$

where the sum in the second part of the equation runs over all (partial) atomic charges q_j in the solvent with radial distances from the ion r_j.

As in Eq. (15) above, the average in Eq. (21) is taken over the configurations of the solvent in equilibrium with the repulsive core of the solute (subscript "0"). This prescription allows one to calculate the interfacial susceptibility from computer simulations with $q = 0$, as is done in this study. Further, the radial projection of the

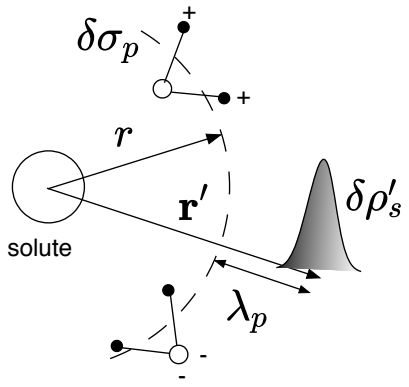

Figure 1. Surface charge density σ_p produced by the water molecules crossing the mathematical surface of the radius r ("+" indicates the partial atomic charge of the hydrogen atoms of the water molecules). Fluctuations of the surface charge density $\delta\sigma_p$ caused by thermal motion correlate over the characteristic correlation length λ_p with the fluctuations of the solvent charge density $\delta\rho'_s = \delta\rho_s(\mathbf{r}')$. These mutual correlations are responsible for the interface susceptibility in Eqs. (21) and (24).

polarization density $P_r(r)$ is calculated in the radial shell between r and $r + dr$ as follows

$$P_r(r) = \frac{1}{4\pi r^2 dr} \sum_{r \le r_j \le r+dr} \mathbf{m}_j \cdot \hat{\mathbf{r}}_j. \qquad (23)$$

Finally, $\delta P_r(r)$ in Eq. (21) are the deviations of $P_r(r)$ from average values in each shell.

Given the obvious non-locality of the dipolar interactions in a polar liquid, Eq. (21) might look misleadingly local, suggesting a possibility to define a local polarization response in the interface. Clarifying the physical meaning of the correlation function in the right-hand side of Eq. (21) seems therefore useful.

The radial projection of the polarization density is also the normal projection of the vector field $\mathbf{P}$ on the sphere of radius r. Consequently, $P_r(r) = \sigma_p(r)$ defines the density of surface charge[30] $\sigma_p(r)$ arising from the mathematical surface cutting through the water molecules crossing the surface and by that creating surface monopoles (Fig. 1). Fluctuations of P_r correspond, therefore, to fluctuations of the surface charge density, $\delta P_r = \delta\sigma_p$. These surface fluctuations correlate with the fluctuations of the molecular charge density $\delta\rho'$ over some correlation length λ_p. The result of these mutually correlated fluctuations, integrated with the weight $1/r'$, is what makes the interface susceptibility function

$$\chi_0(r) \propto \int (d\mathbf{r}'/r') \langle \delta\sigma_p(r) \delta\rho'_s \rangle_0. \qquad (24)$$

The non-locality of the interfacial response is in fact preserved in the correlation function and is ultimately determined by the extent of interfacial charge-charge correlations.

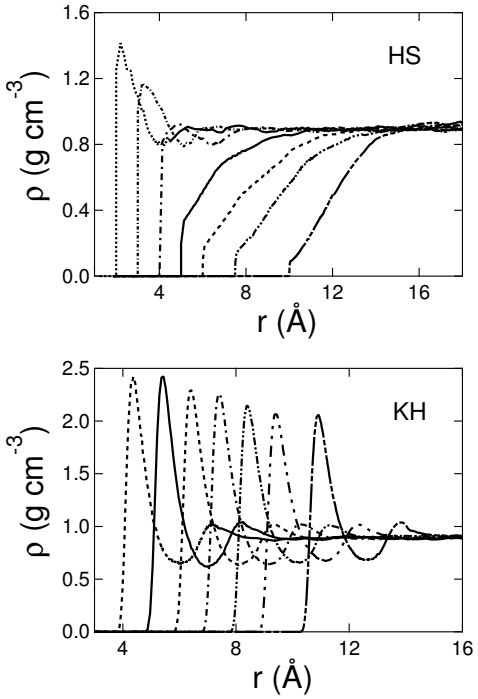

Figure 2. Water density profiles, $\rho(r) = \rho g_{0s}(r)$, around the hard-sphere (HS) and Kihara (KH) solutes as a function of growing size of the solute hard-sphere core ($R_{\rm HS}$ for KH and R_{0s} for HS solute). The density profiles are calculated from MC simulations with a single solute in the simulation cell containing TIP3P water at 298 K (see SM[29] for detail).

III. NUMERICAL SIMULATIONS

Several routes to access the free energy F_0 are available within the linear response. The most widely used and fastest to converge by numerical simulations[1] is through the average potential $\langle\phi\rangle$ [Eq. (22)] of the water solvent in equilibrium with the charge q: $F_0 = (q/2)\,(\langle\phi\rangle_0 + \langle\phi\rangle)$. Here, the equilibrium potential $\langle\phi\rangle$ includes the potential $\langle\phi\rangle_0$ of the spontaneously polarized interface and an additional potential $\langle\phi_q\rangle$ produced by the solvent in response to placing charge q at the center of the solute. It is this second potential that produces the quadratic scaling of the free energy with the ion charge [Eq. (1)] and is our focus here. The use of the average potential to calculate F_0 has its disadvantages when combined with Ewald sums used to treat electrostatic interactions in simulations. Ewald sums require compensating the ion charge q with the uniform background of the opposite charge to neutralize the simulation cell[63,64] and a corresponding correction for the potential of the uniform background is required to calculate $\langle\phi_q\rangle$.

To avoid this somewhat artificial situation of running simulations in a continuum background charge,[65] one can simulate the solute carrying zero charge. The potential $\langle\phi_q\rangle$ can then be calculated from the perturbation theory, leading to the solvation susceptibility in Eq. (1) in the

form[3,4,34]

$$\chi = \beta\langle\delta\phi^2\rangle_0. \quad (25)$$

The simulation cell is neutral in this case and the problem of artificial background charge is avoided. Furthermore, the variance of the potential does not depend on the presence of the charge in the linear response, $\langle\delta\phi^2\rangle_0 = \langle\delta\phi^2\rangle$, and this route can be applied to the calculations involving both neutral and charged solutes because the constant potential of the charged background is subtracted in the variance. We find from our simulations that the equality of two variances is not satisfied for HS solutes carrying positive and negative charges:[2] $\langle\delta\phi^2\rangle_{q<0} > \langle\delta\phi^2\rangle_{q>0}$. The structure of the interface around hard-core objects is strongly modified by introducing even weak attractions,[66] in this case Coulomb solute-solvent interactions, but can be accommodated into the solvation susceptibility through the effective cavity radius depending on the solute-solvent density profile (see below). As the size of the HS core increases, the density profiles of the cations and anions converge and the gap between the corresponding variances narrows.

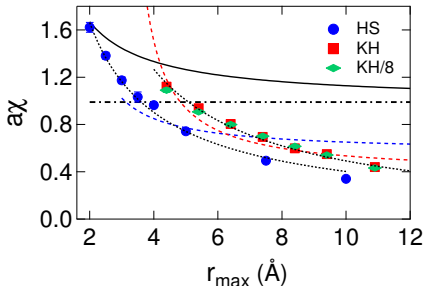

Figure 3. Ion dimensionless solvation susceptibility $a\chi$ from Eq. (1) obtained in MC simulations and different models using the parameters of TIP3P water: $\epsilon = 97$, $\sigma = 2.87$ Å (effective HS diameter), and $m = 2.35$ D. The horizontal dashed line shows the Born result, Eq. (2). The points are results of MC simulations for HS and Kihara solutes with the solute-solvent LJ energy $\epsilon_{\rm LJ} = 3.7$ kJ/mol ("KH") and 8 kJ/mol ("KH/8"). The solvation free energies extracted from MC simulations are multiplied with the distance $r_{\rm max}$ from the solute center to the first maximum of the solute-solvent pair distribution function ($a = r_{\rm max}$). The points in the plot therefore show $-2r_{\rm max}F_0/q^2$, where the solvation free energy F_0 is determined according to Eq. (25). The blue and red dashed lines are fits of the simulation data to the dependence $r_{\rm max}/(r_{\rm max} - \Delta)$ (see text for explanation). The solid line is the calculation with the homogeneous approximation, Eq. (13). The black dotted lines are fits to the power decay $\propto r_{\rm max}^{-\gamma}$ with $\gamma = 0.9$ (HS) and 1.0 (KH).

A. Simulation protocols

The second cumulant route to the solvation free energy [Eq. (25)] was adopted in our Monte Carlo (MC) and molecular dynamics (MD) simulations of solutes of varying size and solute-solvent potential hydrated by TIP3P[67] water at 298 K. The main goal here is to see how the structure of the solute-water interface affects the dependence of χ in Eq. (1) on the solute size. Here, we have significantly extended the range of solute sizes typically studied in the field of ion solvation[4,12,14] to the range of ~ 1 nm when a substantial restructuring of the interface is expected to occur.[68–70] Our goal is also to compare the performance of the homogeneous and local approximations against simulations and to explore the possibility of establishing a measure of the local polarity of the interface that can potentially replace the dielectric constant in the Born equation. We indeed find that this local polarity can be defined in terms of the radial susceptibility $\chi_0(r)$.

A detailed description of the MC/MD simulation protocols is given in SM.[29] Here, we only briefly describe the system setup. Two types of solutes interacting with TIP3P water[67] at 298 K were used in the simulations. The first solute is a HS characterized by the distance of the closest approach R_{0s} of the water solvent to the solute. The size of the HS solute was varied by changing this parameter in the range $R_{0s} = 2-10$ Å. We observed a strong dewetting[68,70] of TIP3P water at $R_{0s} \geq 5$ Å (Fig. 2). Since the dewetting phenomenon is strongly affected by the solute-solvent attraction and might not occur for more realistic solutes of this size,[66] two types of the solute-solvent attractions were introduced. A number of single-charged ($|q| = 1$) anions and cations were simulated. These introduce electrostatic attractions with the interfacial water multipoles oriented along the ion field. These attractions, however, become weaker with increasing the solute size and dewetting still occurs (Fig. S2 in SM[29]).

Real multi-atomic ions always involve solute-solvent dispersion attractions, which typically prevent dewetting of the interface.[66] In order to represent this situation in our modeling, simulations with the Kihara solute-solvent potential[71] were carried out as well. The Kihara potential adds a layer of LJ 6-12 potential to a HS core characterized by the radius $R_{\rm HS}$ (see SM[29]). The extent of solute-solvent attraction can be controlled by the solute-solvent LJ energy $\epsilon_{\rm LJ}$. The size of the solute was varied by changing $R_{\rm HS}$ in the range $1-7.5$ Å. The electrostatic potential of water at the center of the solute was calculated from the MC configurations and used to calculate the potential variance in Eq. (16). Since Kihara potential does not have the problem of discontinuous forces characteristic of HS repulsion, we used the NAMD 2.9[72] software package to calculate $\chi_0(r)$ from Eq. (21) for two Kihara solutes. The susceptibility $\chi_0(r)$ is fundamentally a three-particle correlation function, requiring long trajectories (~ 200 ns) to converge.

B. Solvation free energy

Figure 3 shows the ion solvation susceptibility $a\chi$ in Eq. (1) as a function of the cavity radius for HS and Kihara solutes (the results for anions and cations are given in Fig. S3 in SM[29]). The Born equation, Eq. (2), predicts a constant value, fully determined by the dielectric constant, which is shown by the horizontal dash-dotted line. The homogeneous approximation is shown by the solid line, and it approaches the continuum limit from above with increasing the solute size a, as expected from the general arguments. The calculations were done by applying Eq. (13), in which the longitudinal structure factor from numerical simulations[20,73] of TIP3P water was used.

The points shown in the plot refer to the dimensionless parameter $r_{\max}\chi$ with χ calculated according to Eq. (25) and $r_{\max}$ referring to the first maximum of the solute-solvent pair distribution function. We note that the solvation susceptibility is affected by the nature of the solute-solvent potential (HS vs Kihara), but is less affected by the strength of LJ attraction. The two nearly coinciding sets of points in Fig. 3 refer to the solute-solvent LJ energy of $\epsilon_{\rm LJ} = 3.7$ kJ/mol (squares) and 8.0 kJ/mol (diamonds) in the Kihara potential. They demonstrate low sensitivity of the solvation susceptibility to the strength of solute-solvent LJ attraction.

Since the cavity radius a is an empirical parameter, which does not have to coincide with $r_{\max}$, the Born equation would predict $r_{\max}\chi \propto r_{\max}/(r_{\max} - \Delta)$ (Eq. (3)), where Δ is a distance offset to obtain the cavity radius from $r_{\max}$, $a = r_{\max} - \Delta$. The simulation results do not follow these expectations, as is shown by the dashed lines in Fig. 3 attempting to fit the simulation points. A numerically better fit follows from the power decay $r_{\max}\chi \propto r_{\max}^{-\gamma}$ with $\gamma \simeq 0.9 - 1.0$. We can conclude that the scaling of the solvation susceptibility with the solute size anticipated by the Born equation is not supported by the simulations.

The alternative to the Born equation is the integral form in Eq. (14), which involves the local radial susceptibility $\chi_0(r)$. Equation (21) provides an exact solution for this function, while the local approximation involves simplifications of two levels: the neglect of the spatial extent of dipolar correlations in the hydration shell that leads to Eq. (15), followed by the use of the continuum approximation in evaluating the correlator between radial polarization and the radial dipole moment that leads to Eq. (16). Two MD simulations of Kihara solutes of different size were carried out to access $\chi_0(r)$ and test both approximations.

We first find that $\chi_0(r)$ as calculated from the exact relation in Eq. (21) is an oscillatory function, with oscillations compatible with the density profile around the solute (Fig. 4). This result is consistent with Eq. (16), but the amplitude of oscillations is significantly overestimated by that relation (not shown in the plot). At the same time, the local approximation itself, without the use of the continuum limit in Eq. (16), is a much better representation of $\chi_0(r)$, with only a slight overestimate of the oscillations amplitude (cf. blue and black lines in Fig. 4). This comparison is a strong evidence in support of the local approximation compared to the homogeneous one, suggesting that the focus on the local structure of the hydration shell, in contrast to the bulk-like dipolar correlations, is a better starting point for constructing predictive theories of ion hydration.

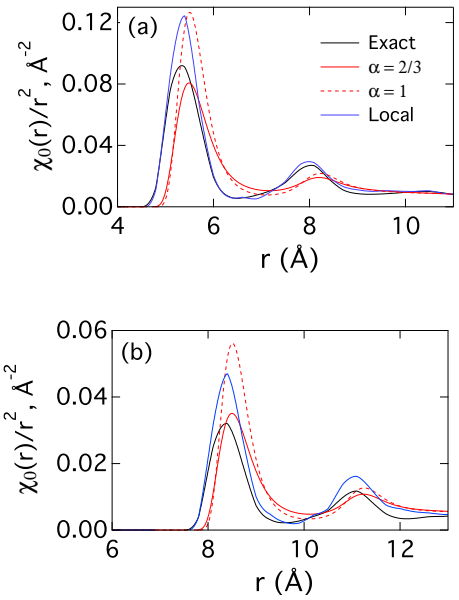

Figure 4. Integrand function $\chi_0(r)/r^2$ in Eq. (14) for Kihara solutes with $R_{\rm HS} = 2$ Å (a) and 5 Å (b). The exact susceptibility function [Eq. (21)] calculated from MD simulations (black lines) is compared to the empirical relation [Eq. (26)] with $\alpha = 2/3$ (solid red lines) and $\alpha = 1$ (dashed red lines). The blue lines indicate χ_0 calculated in the local approximation given by Eq. (15). The labelling of the lines is consistent between panels (a) and (b).

The focus on the solute-solvent density profile to determine the solvation susceptibility as suggested by Eq. (16) is still a useful perspective, which needs to be corrected to provide quantitatively reliable results. A better agreement with simulations can be obtained by taking a fractional power, instead of a square, of the pair distribution function in Eq. (16). This results in the radial susceptibility function in the form

$$\chi_0(r) = \left(1 - \epsilon^{-1}\right) [g_{0s}(r)]^{\alpha} . \qquad (26)$$

Figure 4 shows $\chi_0(r)/r^2$ (the integrand in Eq. (14)) with $\alpha = 2/3$ compared to the MD results. This empirical prescription is used to calculate the effective cavity radius in Eq. (18).

It is important to understand the physical origin of a sublinear scaling of the interface susceptibility function with the density profile of the interface. Allowing long-range, bulk-like dipolar correlations in the interface

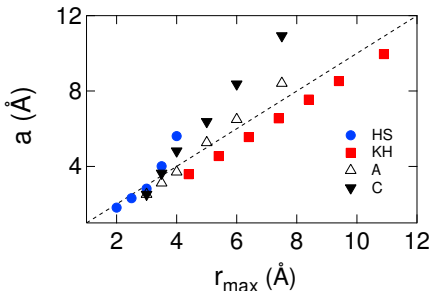

Figure 5. Cavity radius a determined from Eq. (18) plotted against the position of the first peak of the solute-solvent radial distribution function $r_{\max}$. The dashed line is $a = r_{\max}$ line drawn to guide the eye. The simulations points are for hard-sphere (HS), Kihara (KH), hard-sphere anion (A), and hard-sphere cation (C) solutes. $r_{\max} = R_{0s}$ for HS solutes.

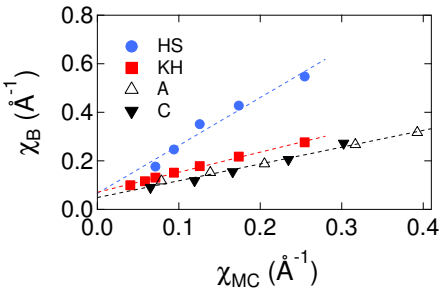

Figure 6. Solvation susceptibility χ (Eq. (1)) calculated from MC simulations as $\chi_{\rm MC} = -2F_0/q^2 = \beta\langle(\delta\phi)^2\rangle_0$ and from the Born equation $\chi_{\rm B} = a^{-1}\left(1-\epsilon^{-1}\right)$ with the cavity radius a calculated from Eq. (18). The results are reported for the hard-sphere (HS), Kihara (KH), and ionic (cations "C" and anions "A") solutes. The dashed lines are linear fits through the points with the slopes 2.0 (HS), 0.8 (KH), and 0.7 (C+A).

leads to $\alpha = 2$ in Eqs. (16) and (26). This result physically implies that the dipolar correlations act cooperatively and enhance the susceptibility in denser parts of the shell characterized by peaks of the radial distribution function. When the correlations between the dipoles are neglected and only a one-particle dipolar response is considered in the perturbation theory, one arrives[58,59] at $\alpha = 1$ in Eq. (26). The sublinear scaling obtained from fitting the simulation data implies that denser parts of the shell significantly hinder one-particle dipolar reorientations and a response weaker than the one-particle one is produced. The linear scaling of the distant-dependent dielectric constant with the density profile ($\alpha = 1$) was noticed previously,[39,74] but this scaling seems to apply better to the approximate, local form of the susceptibility function [Eq. (15)] used in those simulations (cf. blue lines with dashed red lines in Fig. 4).

C. Effective cavity radius

Figure 5 compares the effective cavity radius a calculated from Eq. (18) to the position of the first peak maximum $r_{\max}$ of the solute-solvent radial distribution function. The height of the peak is affected by packing advantages close to a solute of large size, increasing its amplitude, and by the balance between the solute-solvent and solvent-solvent attractions. The existence of the peak implies that the effective cavity radius a is below $r_{\max}$, as is seen for the Kihara solute (red squares in Fig. 5), for which the amplitude of the density peak stays nearly constant with the growing HS core (Fig. 2, lower panel). The situation, however, becomes more complex when the interfacial structure significantly changes with increasing solute size.

This is the case with the HS solutes, where without the surface LJ attraction of the Kihara potential, dewetting of the interfacial water occurs as the solute size increases (Fig. 2, upper panel). Lowering density of the interface results in an upward shift of the cavity radius a, which becomes greater than $r_{\max}$ (blue circles in Fig. 5). HS anions and cations show a weaker dewetting of the interface due to the solute-water attraction (Fig. S2 in SM[29]), but the increase of the cavity radius is still observed as the attraction of the water molecules to the solute becomes weaker with the growing solute size. In addition, the cavity size of the cations (filled triangles in Fig. 5) is consistently greater than the cavity size of the anions (open triangles in Fig. 5). This implies higher in magnitude solvation energies of the anions compared to the cations of the same size, a phenomenon well documented for ion hydration.

The simple and significant outcome of this calculation is that assuming a constant distance offset of $r_{\max}$ to define the cavity radius, such as $a = r_{\max} - \Delta$ (as follows from the MSA and often empirically assumed), has little chance to perform well for a broad range of solute radii and solute-solvent potentials. Figure 5 in fact shows that the offset Δ can be either positive or negative depending on the interaction potential. The Kihara potential might be a fortuitous case when this prescription works relatively well because the interfacial density profile remains almost unchanged with growing HS core due to the specific form of this potential.

The cavity radius from Eq. (18) gives a good account of the free energy change with the solute size. Figure 6 compares the solvation susceptibility $\chi_{\rm MC}$ from MC simulations [Eq. (25)] to $\chi_{\rm B}$ [Eq. (2)] with the cavity radius a given by Eq. (18). The slope of the straight line between $\chi_{\rm B}$ and $\chi_{\rm MC}$ deviates from unity because of the $k \to 0$ approximation for the correlations between the dipoles in the hydration shell used to derive Eq. (18). Nevertheless, the distinction in solvation energies of cations and anions of equal size (Fig. 5) is successfully accommodated in terms of their corresponding cavity radii.

IV. CONCLUSIONS

We have presented here a consistent derivation of the radial dipolar susceptibility of water hydrating a spherical ion. This function is viewed as a microscopic foundation of the distant-dependent dielectric constant of phenomenological models. An exact solution for this function is given in terms of the correlation between fluctuations of the radial polarization density of water with fluctuations of the electrostatic potential created by water at the position of the ion [Eq. (21)]. The susceptibility calculated from numerical simulations shows an oscillatory behavior consistent with the density profile of the interface. This function is empirically approximated by a power law of the solute-water pair distribution function. Oscillations of the interface susceptibility make approximations based on smooth distance-dependent dielectric constants of the interface inconsistent with the exact solution.

The connection between the interface radial susceptibility and the pair distribution function has allowed us to determine the effective cavity radius in the Born expression for the solvation free energy. This connection would not have been possible in the absence of the susceptibility function since developing cavity models by fitting the overall solvation energy is unreliable. The proposed algorithm incorporates the density profile of the interface into the definition of the electrostatic cavity [Eq. (18)]. This expression provides correct scaling of the hydration free energy with the solute size and successfully accounts for different solvation energies of anions and cations of the same size in terms of different density of water in their hydration shells.

ACKNOWLEDGMENTS

This research was supported by the National Science Foundation (CHE-1464810) and through XSEDE resources (TG-MCB080116N).

REFERENCES

[1] J. Åqvist and T. Hansson, J. Phys. Chem. **100**, 9512 (1996).
[2] G. Hummer, L. R. Pratt, and A. E. Garcia, J. Phys. Chem. **100**, 1206 (1996).
[3] G. Hummer, L. R. Pratt, and A. E. Garcia, J. Phys. Chem. A **102**, 7885 (1998).
[4] S. Rajamani, T. Ghosh, and S. Garde, J. Chem. Phys. **120**, 4457 (2004).
[5] R. M. Noyes, J. Am. Chem. Soc. **84**, 513 (1962).
[6] Y. Marcus, *Ion Solvation* (Wiley, 1985).
[7] P. Hünenberger and M. Reif, *Single-Ion Solvation. Experimental and Theoretical Approaches to Elusive Thermodynamic Quantities* (RSC Publishing, Cambridge, UK, 2011).
[8] M. Born, Z. Phys. **1**, 45 (1920).
[9] P. A. Madden and R. W. Impey, Chem. Phys. Lett. **123**, 502 (1986).
[10] D. Kivelson and H. Friedman, J. Phys. Chem. **93**, 7026 (1989).
[11] W. M. Latimer, K. S. Pitzer, and C. M. Slansky, J. Chem. Phys. **7**, 108 (1939).
[12] H. S. Ashbaugh and D. Asthagiri, J. Chem. Phys. **129**, 204501 (2008).
[13] D. Y. C. Chan, D. J. Mitchell, and B. W. Ninham, J. Chem. Phys. **70**, 2946 (1979).
[14] C. S. Babu and C. Lim, *The Journal of Physical Chemistry B*, J. Phys. Chem. B **103**, 7958 (1999).
[15] B. Jayaram, R. Fine, K. Sharp, and B. Honig, J. Phys. Chem. **93**, 4320 (1989).
[16] B. Roux, H.-A. Yu, and M. Karplus, J. Phys. Chem. **94**, 4683 (1990).
[17] B. Linder and D. Hoernschemeyer, J. Chem. Phys. **46**, 784 (1967).
[18] R. M. Lynden-Bell and J. C. Rasaiah, J. Chem. Phys. **107**, 1981 (1997).
[19] P. Vath, M. B. Zimmt, D. V. Matyushov, and G. A. Voth, J. Phys. Chem. B **103**, 9130 (1999).
[20] D. N. LeBard and D. V. Matyushov, J. Chem. Phys. **128**, 155106 (2008).
[21] H. S. Ashbaugh, J. Phys. Chem. B **104**, 7235 (2000).
[22] D. M. Rogers and T. L. Beck, J. Chem. Phys. **129**, 134505 (2008).
[23] M. Paluch, Adv. Colloid Interface Sci. **84**, 27 (2000).
[24] L. R. Pratt, J. Phys. Chem. **96**, 25 (1992).
[25] V. P. Sokhan and D. J. Tildesley, Mol. Phys. **92**, 625 (1997).
[26] L. Horváth, T. Beu, M. Manghi, and J. Palmeri, J. Chem. Phys. **138**, 154702 (2013).
[27] R. C. Remsing, M. D. Baer, G. K. Schenter, C. J. Mundy, and J. D. Weeks, J. Phys. Chem. Lett. **5**, 2767 (2014).
[28] Y. Shi and T. L. Beck, J. Chem. Phys. **139**, 044504 (2013).
[29] See supplementary material at [URL will be inserted by AIP] for details of the simulation protocol.
[30] J. D. Jackson, *Classical Electrodynamics* (Wiley, New York, 1999).
[31] C. G. Gray and K. E. Gubbins, *Theory of Molecular Liquids* (Clarendon Press, Oxford, 1984).
[32] A. A. Milischuk and D. V. Matyushov, J. Chem. Phys. **123**, 044501 (2005).
[33] L. D. Landau and E. M. Lifshitz, *Electrodynamics of Continuous Media* (Pergamon, Oxford, 1984).
[34] T. L. Beck, J. Stat. Phys. **145**, 335 (2011).
[35] J. P. Bardhan, P. Jungwirth, and L. Makowski, J. Chem. Phys. **137**, 124101 (2012).
[36] G. Jeanmairet, M. Levesque, R. Vuilleumier, and D. Borgis, J. Phys. Chem. Lett. **4**, 619 (2013).
[37] H. Gong and K. F. Freed, Phys. Rev. Lett. **102**, 057603 (2009).
[38] X. Song, D. Chandler, and R. A. Marcus, J. Phys. Chem. **100**, 11954 (1996).

[39]V. Ballenegger and J.-P. Hansen, J. Chem. Phys. **122**, 114711 (2005).
[40]O. V. Dolgov, D. A. Kirzhnits, and E. G. Maksimov, Rev. Mod. Phys. **53**, 81 (1981).
[41]J. P. Hansen and I. R. McDonald, *Theory of Simple Liquids* (Academic Press, Amsterdam, 2003).
[42]T. Abe, J. Phys. Chem. **90**, 713 (1986).
[43]B. Mallik, A. Masunov, and T. Lazaridis, J. Comput. Chem. **23**, 1090 (2002).
[44]A. D. Friesen and D. V. Matyushov, Chem. Phys. Lett. **511**, 256 (2011).
[45]A. Ghoufi, A. Szymczyk, R. Renou, and M. Ding, EPL (Europhysics Letters) **99**, 37008 (2012).
[46]H. A. Stern and S. E. Feller, J. Chem. Phys. **118**, 3401 (2003).
[47]D. J. Bonthuis, S. Gekle, and R. R. Netz, Phys. Rev. Lett. **107**, 166102 (2011).
[48]D. J. Bonthuis and R. R. Netz, J. Phys. Chem. B **117**, 11397 (2013).
[49]K. Takae and A. Onuki, J. Phys. Chem. B **119**, DOI: 10.1021/jp510296b (2015).
[50]S. Mukamel, *Principles of Nonlinear Optical Spectroscopy* (Oxford University Press, New York, 1995).
[51]D. V. Matyushov, J. Chem. Phys. **120**, 7532 (2004).
[52]P. Madden and D. Kivelson, Adv. Chem. Phys. **56**, 467 (1984).
[53]F. O. Raineri, H. Resat, and H. L. Friedman, J. Chem. Phys. **96**, 3068 (1992).
[54]T. Fonseca and B. M. Ladanyi, J. Chem. Phys. **11**, 8148 (1990).
[55]G. Stell, G. N. Patey, and J. S. Høye, Adv. Chem. Phys. **48**, 183 (1981).
[56]I. S. Gradshteyn and Ryzhik, *Table of Integrals, Series, and Products* (Academic Press, San Diego, 1994).
[57]L. Onsager, J. Am. Chem. Soc. **58**, 1486 (1936).
[58]J. S. Bader, C. M. Cortis, and B. J. Berne, J. Chem. Phys. **106**, 2372 (1997).
[59]A. Papazyan and A. Warshel, J. Phys. Chem. B **102**, 5348 (1998).
[60]B. U. Felderhof, J. Chem. Phys. **67**, 493 (1977).
[61]J. S. Høye and G. Stell, J. Chem. Phys. **72**, 1597 (1980).
[62]D. V. Matyushov, J. Chem. Phys. **140**, 224506 (2014).
[63]F. Figueirido, G. S. Del Buono, and R. M. Levy, J. Chem. Phys. **103**, 6133 (1995).
[64]G. Hummer, L. R. Pratt, and A. E. García, J. Chem. Phys. **107**, 9275 (1997).
[65]M. M. Reif and P. H. Hünenberger, J. Chem. Phys. **134**, 144104 (2011).
[66]B. J. Berne, J. D. Weeks, and R. Zhou, Annu. Rev. Phys. Chem. **60**, 85 (2009).
[67]W. L. Jorgensen, J. Chandrasekhar, J. D. Madura, R. W. Impey, and M. L. Klein, J. Chem. Phys. **79**, 926 (1983).
[68]D. M. Huang and D. Chandler, Phys. Rev. E **61**, 1501 (2000).
[69]D. Chandler, Nature **437**, 640 (2005).
[70]S. Rajamani, T. M. Truskett, and S. Garde, Proc. Natl. Acad. Sci. **102**, 9475 (2005).
[71]T. Kihara and K. Miyoshi, J. Stat. Phys. **13**, 337 (1975).
[72]J. C. Phillips, R. Braun, W. Wang, J. Gumbart, E. Tajkhorshid, E. Villa, C. Chipot, R. D. Skeel, L. Kalé, and K. Schulten, J. Comput. Chem. **26**, 1781 (2005).
[73]A. A. Milischuk, D. V. Matyushov, and M. D. Newton, Chem. Phys. **324**, 172 (2006).
[74]R. Renou, A. Szymczyk, G. Maurin, and A. Ghoufi, Mol. Simulation **41**, 483 (2014).